The Cockcroft Institute
of Accelerator Science and Technology

Cockcroft-12-15

EXPERIMENTAL CHARACTERIZATION OF A FLEXIBLE IONIZATION MONITOR FOR TRANSVERSE PROFILE MEASUREMENT IN THE USR

Massimiliano Putignano, Dominic Borrows, Carsten P. Welsch
Cockcroft Institute and University of Liverpool, UK

EXPERIMENTAL CHARACTERIZATION OF A FLEXIBLE IONIZATION MONITOR FOR TRANSVERSE PROFILE MEASUREMENT IN THE USR*

Massimiliano Putignano, Dominic Borrows, Carsten P. Welsch
Cockcroft Institute and University of Liverpool, UK

Abstract

For least-interceptive measurement of the transverse profile of antimatter beams in the Ultra-low energy Storage Ring (USR), a flexible monitoring apparatus has been designed at the Cockcroft Institute, UK. The monitor relies on ionization of neutral gas atoms from the primary beam, and subsequent imaging of the ionization products on a Micro Channel Plate position sensitive detector. The flexibility of the apparatus lies in the ability of using, as neutral gas target either the residual gas or a supersonic gas jet target, depending on the requirements of the machine. In this paper we introduce and describe the experimental characterization of the monitor in the residual gas monitoring mode.

INTRODUCTION

Development of low-energy storage rings causes widespread beam diagnostic technologies to become obsolete. In particular preservation of the beam lifetime causes perturbing profile monitoring, such as interceptive foils, to be ruled out [2]. Furthermore, existing non-perturbing techniques such as residual gas monitors can take up to about 100 ms to make meaningful measurements, due to the low residual gas pressure, at the expected operating pressure of around 10^{-11} mbar [3].

A possible solution around these limitations is a neutral supersonic gas jet target, shaped into a thin curtain, and bi-dimensional imaging of the gas ions created by impact with the projectiles. Keeping the curtain at a 45° angle from the impinging direction of the projectiles, and extracting the ions perpendicularly to the jet-projectile beam interaction plane on a position sensitive detector, an image of the projectile beam transverse section is formed on the detector, much like a mirror reflection [3].

This monitor becomes hence the monitor of choice for low-energy, ultra-high vacuum storage rings such as the USR, to be installed at the Facility for Low energy Antiproton and Ion Research, within FAIR, Darmstadt [1].

The experimental setup is also fully suited for applicability as a residual gas monitor, due to the equivalence of the detection systems of the two solutions, which extend also to the area, several centimeters in diameter, interested by the extraction field and imaged on the MCP detector. In its residual gas operating mode, the monitor is best suited for operation at higher pressures in the range $10^{-8} \div 10^{-6}$ mbar, typical of the initial stages of commissioning foreseen for the USR. In this pressure range, the residual gas operating mode provides a robust and less complex solution to profile monitoring, without the need for the additional pumping and mechanical installations needed to operate in the supersonic gas jet mode.

The residual gas operating mode has been experimentally investigated and characterized at the setup assembled at the Cockcroft Institute. In this paper we present this experimental characterization, reporting on sensitivity, resolution and noise as well as reporting example measurements taken on a 10 μA electron beam, controllable spot size and 5 keV energy.

MEASUREMENT TECHNIQUE

The output of a profile measurement is an image captured by the CCD camera focused on the detector phosphor screen. A typical imaged beam profile is shown in Fig. 1.

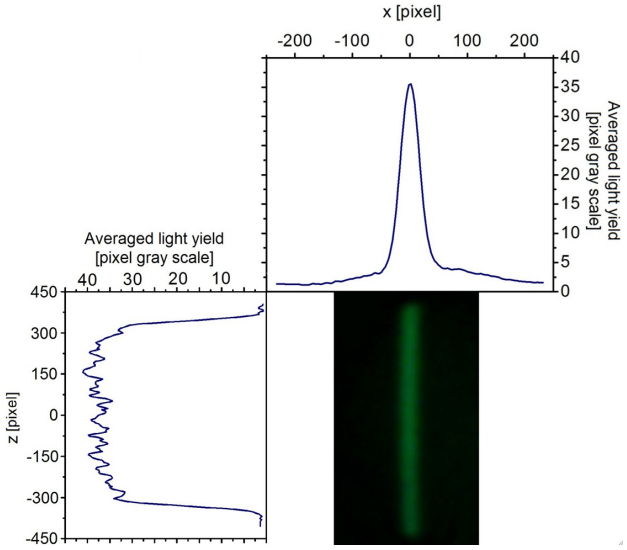

Figure 1: Example of a typical imaged profile of the electron gun beam. The transverse profile follows a Gaussian curve, whilst the longitudinal one is flat, apart from noise. Noise is sensibly higher in the measurement of the longitudinal profile, due to the lower number of pixels included in the averaging.

The 1-dimensional profiles shown in Fig. 1 are obtained by averaging the CCD camera pixel gray scale value over all the pixel rows or columns (depending on the profile axis), imaging the beam. Averaging is preferred to summation in this work so that saturation effects and resolution limits are more readily apparent as the average has the same units of pixel gray scale of the measured observable. This choice only involves a linear transformation, and the two

* Work supported by the Helmholtz Association and GSI Helmholtz Centre under contract VH-NG-328, the EU under contract PITN-GA-215080 and the STFC Cockcroft Institute Core Grant No. ST/G008248/1.

profiles (obtained by average or summation) hence retain the same shape. One profile shows the transverse dimension of the beam, and is therefore Gaussian in shape. The other is instead flat as expected, as there is no charge absorption or emission along the path of the beam and therefore the longitudinal profile is not expected to change. Even in presence of a focusing effect, the longitudinal profile obtained would still be flat: indeed, provided the whole beam is included in it, and not only its central part, the profile is directly proportional to the charge in the beam, which is not changed by focusing or defocusing. By including only the central part of the beam in the profiling average, however, it is possible to see focusing effects reflected in a higher luminosity in the central part of the beam.

EXPERIMENTAL CHARACTERIZATION

Spatial Sensitivity and Resolution

To obtain the sensitivity of the transverse profile monitor, a measurement of σ_{det}, i.e. the beam transverse standard deviation observed on the MCP detector, in terms of σ_{beam}, i.e. the true value of the beam transverse standard deviation as measured directly on a direct hit phosphor screen, was performed. Two sources of error in the measurement of the transverse profile can be identified in the initial velocity of the gas ions, resulting in a drift in the extraction field, and hence a smearing of the formed image, and in the granularity of the MCP detector, indicated respectively with σ_{drift} and σ_{MCP}. A theoretical model for σ_{Det}, which takes into account these two contribution can then can be written as:

$$\sigma_{Det} \;=\; S\sqrt{\sigma^2_{beam} + \sigma^2_{drift} + \sigma^2_{MCP}} \qquad (1)$$

where S is the monitor sensitivity.

Eqn. 1 can be rearranged to yield a linear relation with S^2 as its gradient and $\sigma^2_{drift} + \sigma^2_{MCP}$ being proportional to its intercept:

$$\sigma^2_{Det} \;=\; S^2 \cdot \sigma^2_{beam} + S^2 \cdot (\sigma^2_{drift} + \sigma^2_{MCP}) \qquad (2)$$

The results of the measurements are shown in Fig. 2 so that σ^2_{Det} is plotted versus σ^2_{beam}. 3 different data series have been taken, corresponding to 3 different extraction field values. To perform this measurement, the spot size was varied by using the focus of the electron gun in the range $\sigma_{beam} \;=\; 0.5 \div 3.5$ mm, and the residual gas pressure kept at $5 \cdot 10^{-8}$ mbar to provide good signal visibility.

The results of the best fit regression carried out on the plots of Fig. 2 are reported in table 1.

The sensitivity of the detector is computed through the gradients of the plots in Fig. 2. The data shows that with increasing extraction voltage the sensitivity increases by about 4% when moving from 12 to 30 kV/m.

The resolution of the monitor can be evaluated from the inverse of the sensitivity, resulting in $62 \div 65$ μm, depending on the extraction field used. This value should be compared with the expected beam spot size for the USR before

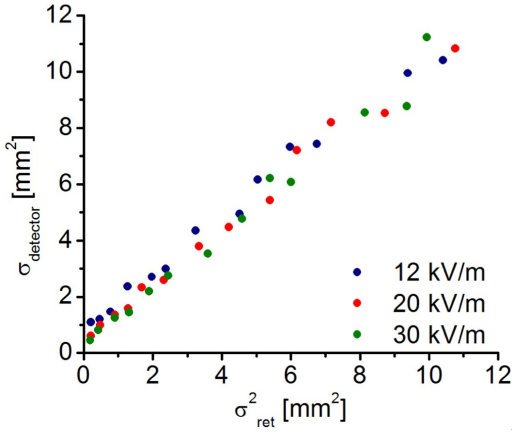

Figure 2: σ^2 of the beam transverse profile as seen on the detector phosphor screen in terms of the same quantity observed on the retractable phosphor screen. Three different measurements are shown, corresponding to different extraction voltages: lower extraction voltages correspond to larger ion drifts.

Extr. Field [kV/m]	**Sensitivity [pix/mm]**	$\sqrt{\sigma^2_{drift} + \sigma^2_{MCP}}$ **[mm]**
12	15.5 ± 0.24	0.99 ± 0.08
20	15.7 ± 0.25	0.71 ± 0.12
30	16.1 ± 0.30	0.48 ± 0.19

Table 1: Detector sensitivity and image spread due to ion drift and MCP as obtained by analysis of the plots in Fig. 2. Confidence intervals calculated by standard errors on the linear regression coefficients are also shown.

cooling, expected to be about 2 cm in diameter at $\pm\, 2\sigma$ at the interaction point. This resolution allows to obtain more than 450 bins for each profile in a 5 cm observation area.

The intercepts of the plots in Fig. 2 are instead linked to the measurement error, as per eqn. 2, and are shown to decrease significantly with increasing extraction field. For use with the beam parameters of the USR they translate in a percentage error of about $0.3 \div 1.3\%$.

Current Sensitivity and Resolution

To define the sensitivity of the monitor with respect to measurement of the signal intensity, the light yield L can be written as:

$$L \;=\; R \cdot A_{Det} \cdot \Delta t \qquad (3)$$

where R is the residual gas ionization rate; A_{Det} is the detector amplification in units of pixel gray scale levels and Δt is the acquisition time, given by the integration time of the CCD camera of 40 ms. A_{Det} includes the contribution of the MCP and the phosphor screen, which can be controlled through the respective bias voltages, but also the light collection efficiency of the camera, given by the combined contributions of CCD sensor sensitivity, camera position and objective lens transparency.

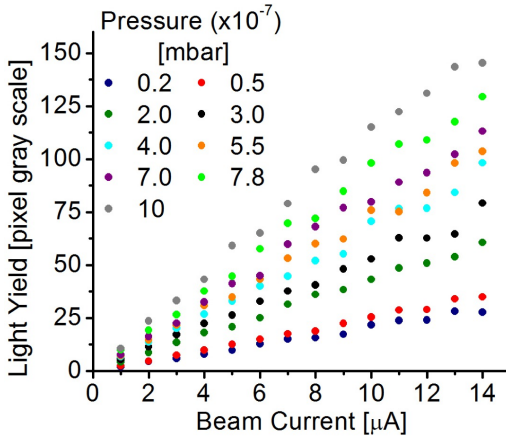

Figure 3: Measurement of integrated light output (in CCD pixel gray scale value) in terms of beam current (x axis) and residual gas pressure (curve parameter), taken for 2 kV MCP and 3kV phosphor screen bias voltages.

Eqn. 3 can be further expanded by expressing R in terms of its components, yielding:

$$L = \sigma(E_{proj})\frac{A_v P_{res.gas}}{RT} l_{obs} \frac{I_{beam}}{q_{proj}} A_{Det} \Delta t \quad (4)$$

where l_{obs} represents the length of the observation region (50 mm) over which ionizations products can be collected on the detector and thus contribute to the signal.

Most of the factors in eqn. 4 are fixed by design and cannot be changed during operation; these can be grouped in a single constant k_d:

$$k_d = \sigma(E_{proj})\frac{A_v l_{obs}}{RT q_{proj}} \Delta t \quad (5)$$

This definition of k_d allows to rewrite eqn. 4 in a form best suited for calculating the monitor sensitivity:

$$L = P_{res.gas} \cdot I_{beam} \cdot A_{Det} \cdot k_d \quad (6)$$

for the monitor presented the constant $k_d = 3.0 \cdot 10^{15}$ [mbar^{-1} mA^{-1}].

The sensitivity S_{cur} of the device in current monitoring mode can be defined as the second derivative of the light output with respect to beam current and residual gas pressure, yielding:

$$S_{cur} = \frac{dL}{dP_{res.gas} dI_{beam}} = A_{Det} k_d \quad (7)$$

To experimentally determine the factor A_{Det} a measurement of the total light output, integrated over the whole beam profile, was carried out for different values of beam current and residual gas pressure, and are shown in Fig. 3:

If the gradients of the $L = f(I_{beam})$ curves are plotted against the corresponding $P_{res.gas}$ values, and the gradient of the obtained curve computed, after dividing for the value of k_d, $A_{Det} = 2.88 \cdot 10^{-6}$ pixel gray scale value amplification.

This value of A_{Det} scales with the bias voltages applied to MCP and phosphor screen. Therefore a maximum value of amplification corresponding to the maximum bias voltage which the detector can support: 2.4 kV for the MCP and 6 kV for the phosphor screen. This yields: $A_{max} = 5.76 \cdot 10^{-4}$ pixel gray scale value amplification. Finally, the maximum sensitivity of the detector can be computed to be:

$$S_{cur} = k_d \cdot A_{max} = 1.73 \cdot 10^{12}\ mbar^{-1}\, mA^{-1} \quad (8)$$

measured in pixel gray scale value per mbar of residual gas pressure and mA of beam current; this corresponds to a resolution $R_{current} = 5.78 \cdot 10^{-13}$ mbar·mA.

The performance of the monitor could be improved if a shorter extraction region was employed. This would result in less drift space, and hence less drift of the created ions. Numerical simulations show that, for a 50 mm wide extraction system, the minimum value permissible for the dimensions of the beam in the USR, the values of $\sqrt{\sigma^2_{drift} + \sigma^2_{MCP}}$ shown in Table 1 could be reduced by a factor of about 3, if the resolution of the MCP itself is neglected. However, below about 30 μm, the spatial resolution of the MCP itself, due to the separation of the single channels, becomes dominant, and no further improvement is possible. On the other hand, the design described allows the flexibility to operate the device in several modes, from residual gas profile monitoring operation for the initial storage ring commissioning, to supersonic jet for profile monitoring at ultra-low residual gas pressures and finally momentum spectroscopy operation mode for collision experiments.

CONCLUSIONS

The experimental characterization of the transverse profile monitor developed and commissioned at the Cockcroft Institute in residual gas operation mode has been presented, demonstrating a spatial resolution of $62 \div 65$ μm and a current resolution of $5.78 \cdot 10^{-13}$ mbar·mA, allowing sampling of the beam profile in the USR with less than 2% transverse profile binning and about 5% current binning.

REFERENCES

[1] C.P. Welsch, et al., "Exploring Sub-Femtosecond Correlated Dynamics with an Ultra-low Energy Electrostatic Storage Ring", AIP Conf. Proc. 796 (2005) p. 266-271

[2] J. Harasimowicz et al, "Beam instrumentation for the future ultra-low energy electrostatic storage ring at FLAIR", Hyperfine Interact (2009) 194:177-181.

[3] M. Putignano et al, "A Fast, Low Perturbation Ionization Beam Profile Monitor Based on a Gas-jet Curtain for the Ultra Low Energy Storage Ring", Hyperfine Interact (2009) 194:189-193.